

Seismic response simulations of bridges considering shear-flexural interaction of columns

Jian Zhang[†] and Shi-Yu Xu[‡]

*Department of Civil and Environmental Engineering, University of California,
Los Angeles, CA 90095, USA*

(Received September 3, 2008, Accepted November 5, 2008)

Abstract. Bridge columns are subjected to combined actions of axial force, shear force and bending moment during earthquakes, caused by spatially-complex earthquake motions, features of structural configurations and the interaction between input and response characteristics. Combined actions can have significant effects on the force and deformation capacity of RC columns, resulting in unexpected large deformations and extensive damage that in turn influences the performance of bridges as vital components of transportation systems. This paper evaluates the seismic response of three prototype reinforced concrete bridges using comprehensive numerical models that are capable of simulating the complex soil-structural interaction effects and nonlinear behavior of columns. An analytical approach that can capture the shear-flexural interacting behavior is developed to model the realistic nonlinear behavior of RC columns, including the pinching behavior, strength deterioration and stiffness softening due to combined actions of shear force, axial force and bending moment. Seismic response analyses were conducted on the prototype bridges under suites of ground motions. Response quantities of bridges (e.g., drift, acceleration, section force and section moment etc.) are compared and evaluated to identify the effects of vertical motion, structural characteristics and the shear-flexural interaction on seismic demand of bridges.

Keywords: column; bridge; seismic response; shear-flexural interaction; hysteretic model.

1. Introduction

The severe damage or collapse of several reinforced concrete bridges in past earthquakes has shown the vulnerability of highway bridges to strong seismic events (Seible and Priestley 1999, Hsu and Fu 2004). As the most critical component in RC bridges, the columns play very important roles in bridges' structural performance and their failures often result in bridge collapse or expensive repair cost. The bridge columns are subjected to multi-directional loadings due to multi-directional earthquake motions and constraints of structural configurations (e.g., skewed or curved bridges etc.). Under the complex load combination of bending, shear, axial load and torsion as result of earthquake shakings, bridge columns will be subjected to yielding, inelastic deformation, and strength and stiffness degradation, all of which imply considerable nonlinear inelastic behavior in the columns. Most of the bridge column damages indicate that insufficient shear or flexural capacity

[†] Assistant Professor, Corresponding author, E-mail: zhangj@ucla.edu

[‡] Graduate Student Researcher, E-mail: xushiyu@ucla.edu

was provided to the columns, which may be resulted from the underestimation of seismic demand or overestimation of bridge capacity. This may due to the fact that current design and analysis methods often treat the different failure mechanisms separately without considering the effects of combined actions, namely the coupling of axial, shear, flexural and torsional responses in the columns. Field evidences as well as laboratory tests have shown that the strength and ductility of columns strongly depend on the combined effects of applied loads as strong interaction exists between them (Saatcioglu and Ozcebe 1989). For example, the flexural strength is affected by the axial force as well as shear force in addition to bending moment while the axial force plays a central role on shear resistance. Neglecting the combined effects will result in over-estimation of lateral load capacity and underestimation of lateral deformation demand. An accurate estimation of seismic demand on bridge columns is required to design the bridges with sufficient seismic capacity. Therefore, it is essential to apply an advanced simulation model to estimate columns' structural behavior considering all failure mechanisms such as axial, shear and flexural failures.

Besides the effects of combined actions on bridge columns, the seismic response simulation of bridges needs to consider the important soil-structure interaction effects, the variation of structural and foundation properties and the input ground motion characteristics. Bridge is an interconnected system, whose seismic response depends on the structural configuration, connection and foundation types. The soil-structure interaction can be quite significant especially at end abutments since the nonlinear behavior of embankment introduced amplified foundation input motion to bridge superstructure and alter the overall system stiffness and damping because of their flexibility and energy dissipation mechanism (Zhang and Makris 2002b). Due to combined actions on bridge columns, the bridges will typically experience higher displacement demand, which in turn will cause higher interaction between the bridge superstructure with foundations and abutments. Therefore, a system level approach is needed to evaluate the seismic demand and capacity of highway bridges with consideration of combined actions and complex dynamic behavior resulted from soil-structure interactions and structural characterization.

In this study, the seismic responses of three prototype RC bridges with various structural details will be investigated using comprehensive numerical models that are capable of simulating the complex soil-structure interaction effects and nonlinear behavior of columns under combined actions. Two hysteretic models developed to describe the nonlinear shear and flexural behaviors of RC columns are implemented as a single user element in commercial software, ABAQUS to model the realistic performance of columns under combined loads. The models are capable of capturing the pinching behavior of RC columns due to the opening and closing of propagating cracks, and the strength deterioration and stiffness softening due to low cycle fatigue. The user element is validated against cyclic loading tests as well as dynamic shake table tests of bridge columns and shown to provide excellent prediction of nonlinear column behavior under combined axial-shear-flexural loadings. The numerical models of three prototype bridges are established including stick models of superstructure, nonlinear column elements with and without considering the shear-flexural interaction and equivalent linear springs and dashpots representing soil-structure interactions at end abutments and column bases. The nonlinear time history analyses are conducted on the prototype bridges when subject to a suite of multi-directional ground motions. The response quantities including column drift, acceleration, section force and section moment etc. are derived and compared to evaluate the effects of ground motion input, structural characteristics and shear-flexural interaction on the seismic demands of bridges at system level. The study demonstrates that the seismic displacement demand of bridges may be underestimated by neglecting the shear-flexural

interaction and the local behavior of bridge columns plays a crucial role in the seismic performance of entire bridge.

2. Modeling shear-flexural interaction of columns

2.1 Deficiency of current prevailing numerical models

Numeric models for RC columns in the past have focused primarily on inelastic flexural behavior and usually decoupled with axial, shear, and torsion behavior. For flexural behavior, the traditional section analysis or the fiber model (with consideration of axial-flexural interaction) in one-dimensional stress field gives acceptable predictions in terms of ultimate strength and yielding displacement (Mostafaei and Kabeyasawa 2007). The shear and torsion behavior are often modeled with a linear decoupled spring in many analysis software packages. This approach appears to be inadequate for modeling the columns dominated in shear or shear-flexural behavior.

Ozcebe and Saatcioglu (1989) reported that shear displacement can be significant even if a RC member is not governed by shear failure. They also indicated that RC members with higher shear strength than flexural strength do not guarantee an elastic behavior in shear deformation. Based on their observation, RC members controlled by flexural behavior (as is the case in most of the current RC design codes) may still have significant shear displacement which goes into the inelastic stage and thus should not be left ignored. ElMandooh Galal and Ghobarah (2003) further pointed out that the dynamic variation of axial force in RC columns will cause significant change in the lateral hysteretic moment-curvature relationship and consequently the overall structural behavior. Hence, in a good nonlinear RC element model, the axial and lateral behaviors should be coupled together.

Two common modeling techniques for nonlinear analysis of RC columns are examined to evaluate their accuracy. Fig. 1(left) compares the experimental results (solid blue lines) of column test TP-021 (Yoneda *et al.* 2001) and the simulated results (dotted red lines) from a commercial FE program, ABAQUS, using the Timoshenko beam elements with nonlinear moment-curvature relationship and a constant shear stiffness. Fig. 1(right) compares the experimental results (solid

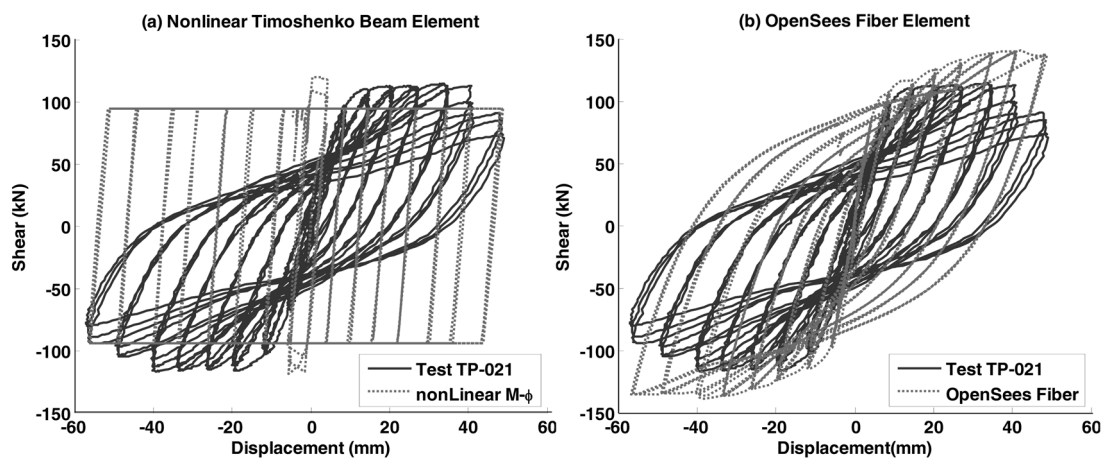


Fig. 1 Analytical hysteretic responses using nonlinear Timoshenko beam and fiber element for TP-021

Table 1 Geometry, reinforcement, material properties, and applied load of examined column tests

Column Index	Column Size (mm)	Column Height (mm)	Number of Steel Rebars	Longitud. Steel Diameter (mm)	Transverse Steel Diameter (mm)	Longitud. Reinforce. Ratio	Transverse Reinforce. Ratio	f_y (MPa)	f_c' (MPa)	Axial Load (kN)	Axial Load Ratio
TP-021	400 circ.	1350	12	16	6	1.89%	0.26%	374	30.0	185	5.0%
TP-031	400×400	1350	20	13	6	1.58%	0.79%	374	22.9	470	12.8%
TP-032	400×400	1350	20	13	6	1.58%	0.79%	374	23.0	-170	-4.6%
PEER-121	606.6 circ.	1828.8	28	19.05	6.4	2.73%	0.89%	441	34.5	911.84	9.0%
PEER-122	606.6 circ.	4876.8	28	19.05	6.4	2.73%	0.89%	441	34.5	911.84	9.0%
UNR-9F1	406.4 circ.	1828.8	20	12.7	6.35	1.95%	1.00%	448	37.4	355.86	10.0%

blue lines) of the same column and the simulated results (dotted red lines) from an open source finite element analysis program, OpenSees (documented by Mazzoni *et al.* 2006), using the force-based fiber element formulation aggregated with a linear elastic shear modulus. Details of column TP-021 is summarized in Table 1 shown above. It is observed that the result from the first model by capturing the nonlinear flexural behavior of columns alone but neglecting the stiffness degrading and so forth, is far away from the realistic column response while the second model by capturing the axial-flexural interaction, provides a much improved prediction yet still fails to capture the often observed pinching behavior and the strength deterioration due to cyclic loading reversals.

2.2 Shear-Flexural Interaction (SFI) model of columns

To mend for the deficiencies in the current models, an analytical approach is developed to include the nonlinear SFI. This approach couples the axial force, shear force, and bending moment at the section level, similar to the fiber section formulation, and produces much improved results. The basic idea is to introduce the SFI into the analytical approach through the primary curves (or backbone curves), which can be perceived as the constitutive law of the RC element. The interaction between axial load, shear force and bending moment is incorporated by the primary curves considering the combined effects and by the requirement of global and local equilibrium at any given time. The proposed approach essentially belongs to the concentrated plastic hinge model, which is empirical and approximate. But it is relatively easy to be implemented and computationally efficient compared to the spread plastic hinge model and the fiber model.

The total primary curve of a column is equivalent to its monotonic force-displacement relationship under the combined loads, and it defines the envelope of hysteresis loops of the column. After separating the shear displacement from the flexural deformation, the total primary curve is broken into shear and flexural primary curves. The decoupled primary curves are then serves as the boundaries for shear and flexural hysteretic reloading and unloading loops of the member and will control the behavior of the RC members. The primary curves can be derived from Modified Compression Field Theory (MCFT) (Vecchio and Collins 1986), which takes into account the compatibility condition, equilibrium condition, and stress-strain relationship when subject to combined axial, shear and bending loads. Fig. 2 describes the general procedure according to MCFT to obtain the primary curves. Given the geometry of the target RC section, the reinforcement configuration, the material properties, and the applied external loads, MCFT can yield the moment-curvature ($M-\phi$) and the shear force-shear strain ($V-\gamma$) relationships of the section subject to the

7% and 93% of the column total lateral deflection, respectively. This assumption is also consistent with the previous finding that the contribution of the shear deformation is less than 10% of the total deformation for a properly designed column (Lehman and Moehle 2000). However, shear deformation can be significant for older columns with poor reinforcement details and it can increase to approximately 40% of total displacement at larger displacement ductility level (Sezen 2008). The user element developed herein is able to consider the larger contribution of the shear deformation easily under the same framework. Upon establishment of primary curves, the cracking loads (V_{cr} and M_{cr}) and yielding loads (V_y and M_y) must be determined to enable the unloading and reloading rules. Cracking load is defined as the point on the primary curve where the strain of the outer most tensile concrete fiber exceeds the concrete crack strain; and yielding load is the point where the stretching rebars first yield.

Two hysteretic models developed by the authors (Xu and Zhang 2008) are adopted in this study to describe the nonlinear shear and flexural responses of reinforced concrete columns subjected to shear force and bending moment reversals. The models are based on the nonlinear shear hysteretic element originally proposed by Ozcebe and Saatcioglu (1989) with several improvements on unloading and reloading rules (Xu and Zhang 2008) to enable successful implementation in standard displacement based finite element framework. Ozcebe and Saatcioglu's model were originally established by statistic regression of experimental data, and it is later revised and calibrated by the authors to allow for possible larger ductility levels, to improve numerical stability, and to expand it to the flexural responses. The detailed model description and implementation can be found elsewhere (Xu and Zhang 2008). The hysteretic shear element describes the nonlinear cyclic behavior such as pinching, strength deterioration and stiffness softening under shear reversals using the above-described shear force to shear displacement ($V-\Delta_s$) primary curve and a set of rules for unloading and reloading branches under cyclic loading. Under the same framework, a hysteretic flexural element is also developed on the same basis with modified unloading and reloading rules specific to bending moment reversals (Xu and Zhang 2008). The primary curve of the flexural hysteretic model defines the nonlinear moment to rotation angle ($M-\theta$) relationship obtained by the procedure described above. The proposed hysteretic flexural and shear models consider the effects of axial load variation on the lateral hysteretic responses, and the unloading and reloading rules are governed by axial load ratio, current force level (shear or moment), current displacement level (shear displacement or rotation angle) and numbers of loading cycles subjected to maximum deformation level. They are implemented as a single user element in ABAQUS. By incorporating these improved unloading and reloading rules, the user element is able to predict realistic behavior of columns very well, including experimentally observed stiffness degradation and pinching of hysteresis loops, as demonstrated by the model verification in the next section.

Shear force and bending moment in this approach are coupled together through their primary curves, and they keep interacting with each other in the hysteretic responses because the global and local equilibrium must be held at any time. If the inflection point of a RC column is known (or simply assuming to be at the mid height of the column), the column can be broken at its inflection point into two cantilever columns and simulated by a rigid bar and a combination of flexural sub-elements (F-UELs) and shear sub-elements (S-UELs), as demonstrated in Fig. 2. The primary curves for the upper and lower springs can be the same if the inflection point is at the middle of the column, or can be different if not. To apply this SFI scheme in a MDOF system under transient analysis, the mass of the bridge column must be lumped to its two ends such that the assumed moment and shear force distribution along the column can be held (that is, $M=Vh$, at the top and

bottom sections). This additional requirement will affect the accuracy of the transient analysis, however, by doing so the captured deformed shape will always be the first vibration mode of the cantilever column thus yielding a conservative estimation of displacement demand in the bridge system analyses.

2.3 Model implementation and verification

The hysteretic model described above has been implemented as a user element (UEL) in the commercial finite element analysis software, ABAQUS. For a given column section, the total primary curve is obtained using Response-2000 software, then broken into shear and flexural primary curves according to the proportion ratios (i.e., 7% and 93% in this paper) of shear and flexural deformations or by integrating the shear strains and curvatures along the length of the column as illustrated in Fig. 2. The primary curves are input into the user element along with the critical points for cracking and yielding and the constant axial force ratio. It should be noted that the MCFT, incorporated into Response-2000, is a force-based approach which will stop once the peak strength of the section is reached (i.e., starting to undergo some softening or reaching the yielding platform). To estimate the descending branch of the primary curves, empirical equations for flexural and shear displacement can be used as alternatives (Sezen 2008). The user element allows a displacement controlled analysis with an input displacement time history.

To validate the user element, comparisons of the hysteretic loops under both static cyclic pushover tests and dynamic shake table tests have been made. Table 1 summarizes the geometry, reinforcement, material properties, and applied axial load of the tested column specimens used for validation in this paper. The first five are from static cyclic pushover experiments while the last one is from a shaking table test. The specimens TP-031 and TP-032, tested by Sakai and Kawashima (2000), have identical geometry and reinforcement details but with different axial loads (12.8% compression for TP-031 and 4.6% tension for TP-032 respectively). The aspect ratio is about 3.375 for these two specimens indicating moderate shear-flexural interaction. Fig. 3 compares the computed cyclic shear force-column tip displacement loops (dotted red lines) of column tests TP-

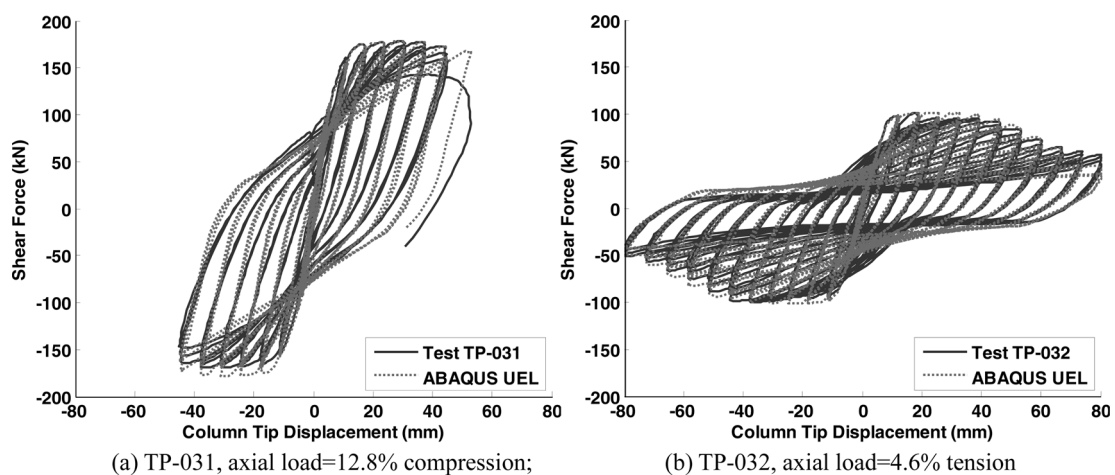


Fig. 3 Comparison of predicted and experimental cyclic responses of columns TP-031 and TP-032 under different axial loads

031 and TP-032 using the shear-flexural interaction user element with the experimental loops (solid blue lines). The experimental results indicate that the variation in axial force has a significant effect on the lateral hysteretic response of RC columns. The small tension force significantly reduces the

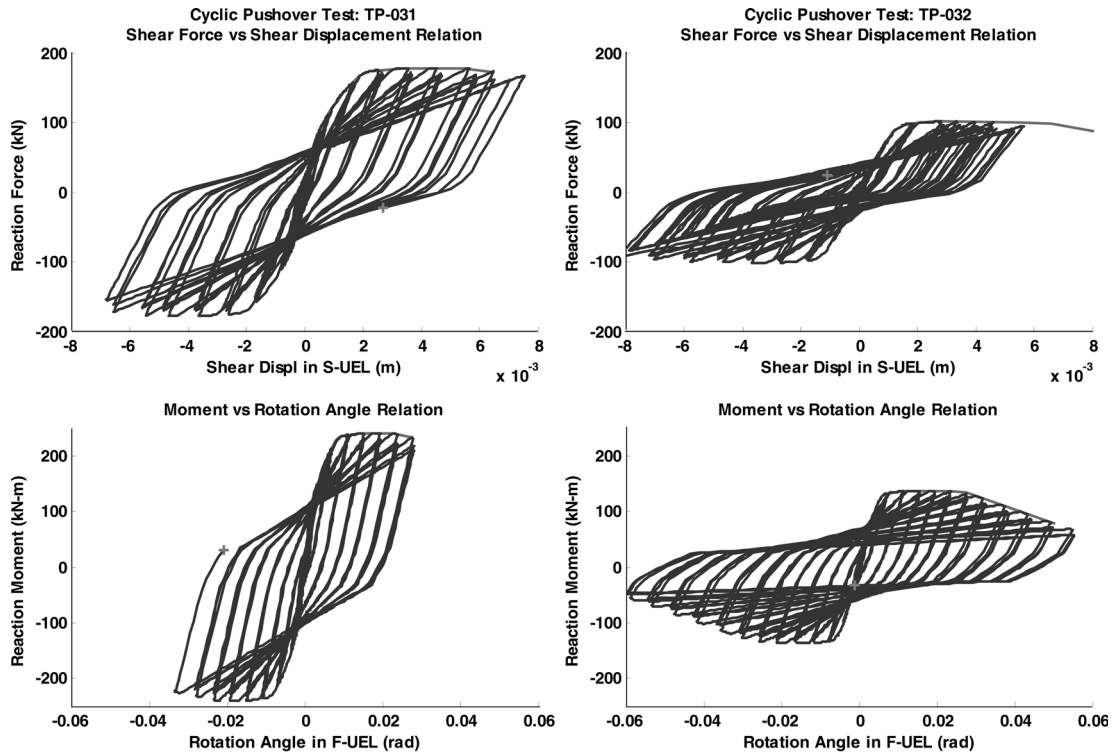


Fig. 4 Shear and flexural hysteretic responses of columns TP-031 (left) and TP-032 (right)

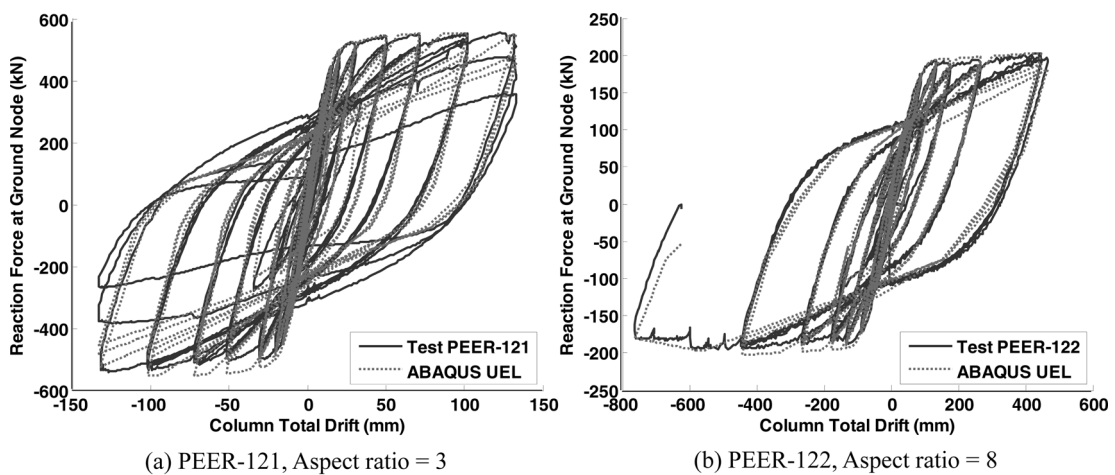


Fig. 5 Comparison of predicted and experimental cyclic responses of columns PEER-121 and PEER-122 with different aspect ratio

ultimate capacity of the columns. The excellent comparison between the computed and the experimental results shows that the developed analytical approach is able to accurately model the nonlinear response as well as the strength degradation and pinching behavior due to the cyclic loading with various axial loads. Fig. 4 displays the shear and flexural hysteretic responses of these two columns. It is seen that the axial load variation affects both the shear and flexural response significantly in the proposed analytical approach.

Fig. 5 compares the computed cyclic shear force-total displacement loops (dotted red lines) of column tests PEER-121 and PEER-122 (Calderone *et al.* 2000) using the user element with the experimental loops (solid blue lines). These two columns are essentially identical to each other except the aspect ratio (i.e., height/diameter ratio). The aspect ratio of the former is 3, which will demonstrate higher level of SFI; and the latter is 8, which is primarily flexural dominant. The results show that the user element is able to capture the responses of either shear or flexural dominant columns very well.

Dynamic validation of the user element is demonstrated in Fig. 6 by comparing the predicted displacement and shear force time history as well as hysteretic loops (dotted red lines) of the column 9F1 with the experimental data (solid blue lines) obtained in a shake table test program conducted at the University of Nevada, Reno (Laplace *et al.* 1999). In the shake table test program, the column specimen 9F1 is subject to multi-event of earthquakes with increasing motion intensity ranging from 0.33 to 4.0 times the ground motion of the 1941 El Centro earthquake record. The column exhibited a flexural-dominated response and experienced complete collapse at the end of the test program. Four different modes were observed at failure, including the longitudinal bar buckling,

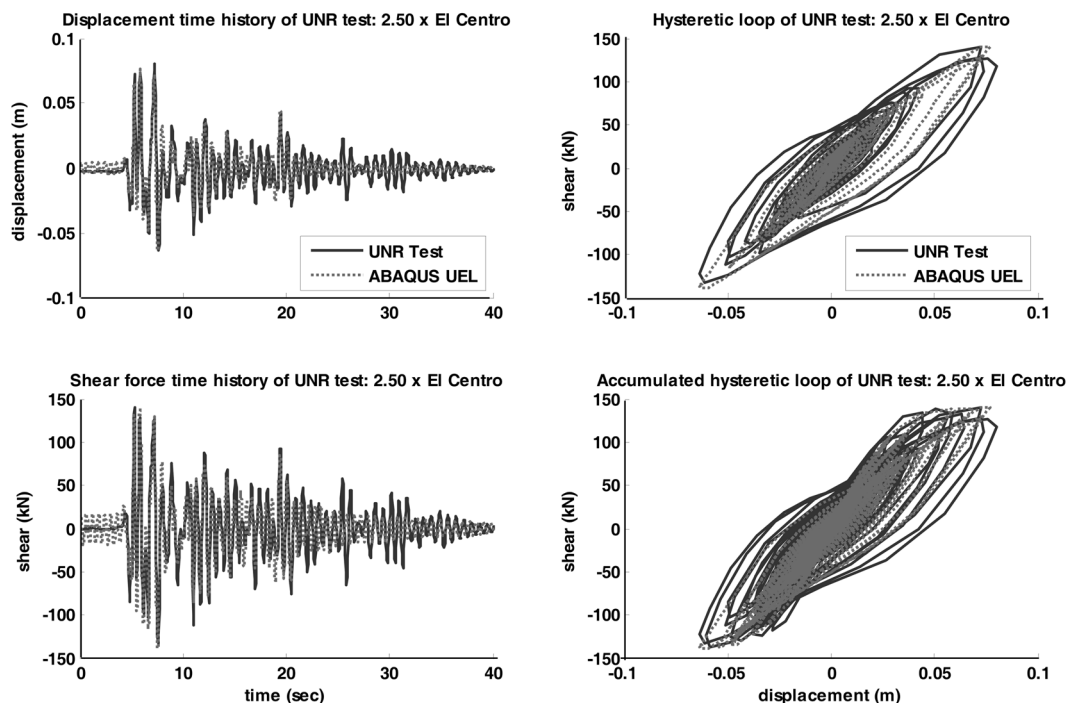


Fig. 6 Comparison of predicted and experimental dynamic responses of column 9F1 under seismic shaking of El Centro earthquake

longitudinal bar fracture, confinement bar fracture and instability due to P- Δ effect. The simulation was also conducted sequentially with the increasing intensity of the earthquake input motion. The numerical predictions at each intensity level are very close to the experimental results. The comparison presented here is the sixth stage of the shake table test whose intensity is 2.5 times the original El Centro earthquake record. At this stage, the column exhibited a spall region of 3 inch tall at the base of the column. The good agreement between the predicted and experimental response again validates that the user element is capable to model the dynamic shear-flexural interaction behavior of columns.

3. Seismic responses of bridges considering shear-flexural interaction

Bridges are interconnected system with huge superstructure, large foundations, and massive surrounding soil, such that the simulation of bridge responses should be done at the system level and that the accuracy of the simulation depends greatly on the sophistication of the numerical model adopted, the characteristics of input ground motions, and the correct modeling of the interaction between the bridges and their surrounding environment (soil-structure interaction, SSI). Most of the column damage observed in past earthquakes indicates that insufficient shear or flexural capacity was provided to the columns, which may be resulted from the underestimation of seismic demand. The two main causes of the underestimation of seismic demand is neglecting soil-structure interaction for the system level response of bridge (Zhang and Makris 2002b) and neglecting the effect of combined actions in numerical models of columns. As discussed in the previous section, the vertical load has significant influence on both shear and flexural responses of columns. The vertical component of ground motions could introduce the variation of axial load inducing prominent pinching behavior and subsequently resulting in larger horizontal deformation (Saadeghvaziri and Foutch 1991). Given the above considerations, the seismic evaluation approach of bridges should include the criteria for selection of ground motions (representative of the possible future excitations caused by the dominant adjacent faults of the site), the consideration of the soil-structural interaction at the bridge abutments and foundations, the modeling of the whole bridge systems, and the modeling of nonlinear behavior of column elements with consideration of the effects of combined actions and loading history.

The structural characteristics of bridges, such as geometry, force resisting, and energy dissipation mechanism, can directly affect their dynamic response under earthquakes. In this study, three prototype bridges with various structural details are selected and examined. Their detailed structural characteristics and column cross section profiles are listed in Table 2 and Table 3 respectively. Bridge #4 is one of the design examples published by FHWA (1996) representing a typical old RC bridge design with a fundamental period around 0.8s. It is a three-span continuous skewed bridge with two-column integral bents and seat type abutments. The column bents are pinned at base and supported on spread footings. The pinned connection is typically used in California to limit the loads transferring to the foundation. For this bridge, the load along the transverse direction can be resisted by the column bents and abutments (before shear keys broken) while the load along the longitudinal direction will be resisted by the column bents only due to the free movement at abutments. Bridge #8 is selected from MCEER/ATC 49-2 (2003) report representing a new design with fundamental structural period of 1.6s. It is a five-span continuous bridge with stub abutments and two-column integral bents. The column bents are monolithically connected with the supporting

Table 2 Structural characteristics of the three prototype bridges

Structural Characteristics	FHWA Design Example #4 Bridge #4	FHWA Design Example #8 Bridge #8	Mendocino Avenue Overcrossing Bridge Mendocino (1963)
Span Length	Three-span continuous	Five-span continuous	Uneven, four-span continuous
Total Length	320 ft long	500 ft long	302 ft long
Pier Type	Two-column integral bent, monolithic at column top, pinned at base	Two-column integral bent (uneven heights), monolithic at column top and base	Single column variable height, monolithic at column top and base
Abutment Type	Seat	Stub abutment with diaphragm	Monolithic
Foundation Type	Spread Footing	Pile Group	Pile Group
Expansion Joints	Expansion bearings & girder stops (shear keys)	Expansion bearings & girder stops	Expansion bearings & girder stops
Force Resisting Mechanism	[Longitudinal] intermediate bent columns & free longitudinal movement at abutments	[Longitudinal] intermediate bent columns and abutment backfill	[Longitudinal] intermediate columns and abutment backfill
	[Transverse] intermediate bent columns & abutment backfill	[Transverse] intermediate bent columns and abutment backfill	[Transverse] intermediate columns and abutment backfill
Plan Geometry	30° skewed bents & abutments	Straight	Straight
Natural Period	~0.8 sec	~1.6 sec	~0.4 sec
Design Method	Old design	New design	Old design

Table 3 Geometry, reinforcement, material properties, and design axial load of prototype bridges

Bridge	Column Size (mm)	Number of Steel Rebars	Longitud. Steel Diameter (mm)	Transverse Steel Diameter (mm)	Longitud. Reinforce. Ratio	Transverse Reinforce. Ratio	fy (MPa)	fc' (MPa)	Axial Load (kN)	Axial Load Ratio
#4	1219.2 circ.	34	35.81(#11)	15.9(#5)	2.93%	0.63%	414	27.6	2927	9.09%
#8 (Bent 3)	1219.2 circ.	20	32.26(#10)	15.9(#5)	1.4%	0.68%	414	27.6	3612	11.2%
Mendocino	1828.8 circ.	26	35.81(#11)	12.7(#4)	1.00%	0.083%	276	20.7	2803	5.16%

pile foundation. For this bridge, both column bents and abutments will contribute to the load transferring along longitudinal and transverse directions. Bridge Mendocino is a real bridge in California, which was also designed based on old design and constructed in 1963. It is a four-span continuous bridge with single columns that have uneven heights and monolithic abutments. Similar to Bridge #8, both columns and abutments resist the earthquake load collectively. The fundamental period of this bridge is about 0.4s. As shown in Table 2, the three prototype bridges are similar but offer good comparison because of their distinctive structural details. They represent the typical highway bridges exist in current bridge inventory in United States.

3.1 Ground motion selection

To conduct seismic evaluation, either the synthetic ground motion records or some groups of

earthquake records selected from the past earthquake database must be provided. However, different earthquake motions will have different duration, frequency content, and magnitude. Hence the input ground motions for dynamic analysis should not be chosen arbitrarily. The general criteria are that the synthetic or selected ground motions must be representative of the specific site and that the variation of earthquakes should be preserved. In this paper, the later approach is used and the ground motion selection and re-scaling criteria adopted is the one suggested by Goulet *et al.* (2007).

It is assumed that all three prototype bridges are located at the Bulk Mail site in Los Angeles (Goulet *et al.* 2007), at which the soil is characterized as NEHRP soil category D with an average shear wave velocity of 285 m/s. The uniform hazard spectra for seven different hazard levels at this site are obtained through Probabilistic Seismic Hazard Analysis (PSHA) and shown in Fig. 7 (left). The numbers inside the parenthesis are the return periods of earthquakes related to each hazard level. Ground motions were selected to be compatible with the mean uniform hazard spectra and consistent with the site conditions. The ground motions critical to hazard level of 2% probability of exceedance in 50 years (Bin 4) is considered in this study. Rescaling of the earthquake records were conducted to maintain the average spectra response of selected ground motions equal to the uniform hazard spectra at a target spectral period. Fig. 7 (right) plots the acceleration spectrum of twelve selected ground motions related to the hazard level of 2% in 50 years at a target period of $T_1 = 0.5s$ in Bin 4 and their average acceleration spectrum. It is observed that the ground motions in Bin 4, although different, are able to maintain the hazard spectra at the target period. Based on this selection approach, both the site-specific characteristics and the uncertainty of earthquake nature are maintained. It is noted that when target period is different, the motions selected based on PSHA and their scaling factors could be different in order to reflect the uniform hazard curve at the sites. In this study two suites of motions are selected for target period of $T_1 = 0.5s$ and $T_1 = 1.5s$. They are listed in Tables 4 and 5 respectively along with their scaling factors. The Bridge #4 and Bridge Mendocino will be subject to the motions listed in Table 4 while the Bridge #8 will be subject to those listed in Table 5 based on their fundamental periods.

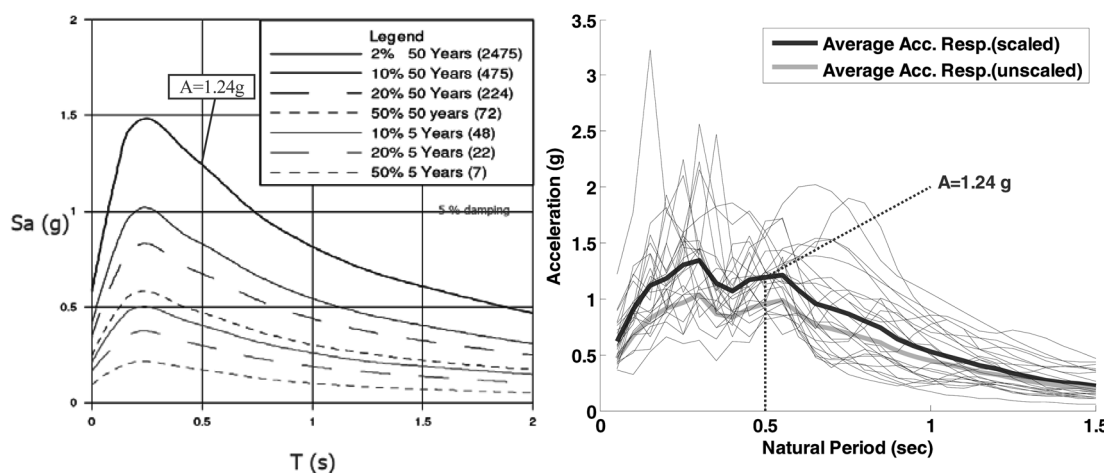


Fig. 7 (left) Mean uniform hazard spectra for the LA Bulk Mail site (Goulet *et al.* 2007), (right) Average acceleration spectrum of Bin4 earthquakes (scaled & unscaled)

Table 4 Ground motions selected for target period of $T_1 = 0.5$ sec

Earthquake	Station	Peak Ground Acceleration (g)			Scaling Factor	
		Horizontal X	Horizontal Y	Vertical		
1987 Whittier Narrows	Studio City – Coldwater	0.177	0.231	0.067	2.79	
1987 Whittier Narrows	N. Hollywood	0.101	0.250	0.059	3.42	
1987 Whittier Narrows	Santa Fe Springs	0.336	0.378	0.206	1.20	
1987 Whittier Narrows	Rancho Los Cerritos	0.159	0.189	0.083	2.84	
Bin 4 (Hazard Level = 2% in 50 years)	1994 Northridge	90013 Beverly Hills	0.416	0.516	0.326	0.74
	1992 Cape Mendocino	Rio Dell Overpass	0.249	0.529	0.131	1.57
	1987 Whittier Narrows	Campton - Castlegate	0.297	0.333	0.137	2.10
	1986 Chalfant Valley	Zack Brothers Ranch	0.447	0.400	0.321	1.04
	1983 Coalinga	Pleasant Valley P.P.	0.592	0.551	0.293	0.89
	1992 Cape Mendocino	89156 Petrolia	0.586	0.662	0.163	1.06
	1994 Northridge	Sepulveda VA Hospital	0.532	0.669	0.467	0.79
	1986 N. Palm Springs	Whitewater Trout Farm	0.492	0.612	0.471	1.04

Table 5 Ground motions selected for target period of $T_1 = 1.5$ sec

Earthquake	Station	Peak Ground Acceleration (g)			Scaling Factor	
		Horizontal X	Horizontal Y	Vertical		
1984 Morgan Hill	Hollister City Hall	0.071	0.071	0.118	5.39	
1987 Whittier Narrows	Fletcher Drive	0.171	0.213	0.103	6.11	
1983 Coalinga	Parkfield – Fault Zone	0.282	0.274	0.097	1.87	
1986 N. Palm Springs	5070 N. Palm Springs	0.594	0.694	0.435	2.64	
Bin 4 (Hazard Level = 2% in 50 years)	1979 Imperial Valley	6621 Chihuahua	0.270	0.254	0.218	3.11
	1986 Chalfant Valley	Zack Brothers Ranch	0.447	0.400	0.321	2.02
	1994 Northridge	90013 Beverly Hills	0.416	0.516	0.326	1.07
	1999 ChiChi Taiwan	HWA011	0.102	0.089	0.039	2.71
	1999 ChiChi Taiwan	KAU020	0.078	0.055	0.02	3.15
	1999 ChiChi Taiwan	HWA013	0.118	0.142	0.064	2.57
	1999 Kocaeli Turkey	Ambarli Termil Santrali	0.249	0.184	0.079	2.32
	1971 San Fernando	Palmdale Fire Station	0.121	0.151	-	4.18

3.2 Soil-structural-interaction modeling of bridges

Soil-structure-interaction (SSI) has long been recognized as one of the essential factors affecting the dynamic response of the bridges under earthquake shaking (Stewart *et al.* 2004). The analysis of SSI effects requires the system to be extended from the structure itself to include the whole structure-foundation-soil system. The SSI effects mainly include the flexible foundation effects, foundation damping effects and kinematic effects. In this study, equivalent linear springs and

dashpots are used to model the first two effects of SSI. Although simple, the equivalent linear springs and dashpots can provide sufficient accuracy for practical purpose (Wolf 1997). The kinematic effects are neglected in this paper since they are generally insignificant for pile foundations and shallow foundations for most earthquake motions. The shear wedge model developed by Zhang and Makris (2002a) is adopted here to derive the spring and dashpot constants for abutments. The analytical solution by Makris and Gazetas (1993) is used to derive the spring and dashpot constants for pile groups taking into account the group interaction effects. The dynamic impedances of shallow foundations as summarized by Gazetas (1991) are used to derive their spring and dashpot constants.

3.3 Structural modeling of bridges

To reduce the computational cost while still maintaining the critical structural characteristics, the stick model, which is a 3d single-lined beam-column frames corresponding to the geometry of centerlines of bridges, is used to model three prototype bridges considered in this study. Major components of the stick model of a bridge include the deck (box girder), the cap beams (for bent bridges), the columns (piers), the footings, foundations, and the abutments. Linear beam elements are used for bridge decks, cap beams and footings while the nonlinear beam elements (nonlinear $M-\phi$ model) or user element with shear-flexural interaction effects are used for modeling columns. Fig. 8 depicts the numerical models of three prototype bridges along with their notable structural details. An imaginary bridge revised from the Bridge Mendocino by replacing the original single-column design with the bent-column design to investigate the effect of column type, is also shown in Fig. 8. Fig. 9 plots the first two natural frequencies and modes of the prototype bridges using the stick models generated in ABAQUS. The natural modes and natural frequencies for Bridges #4 and #8 obtained in ABAQUS are in good agreement with the values reported in the design examples (FHWA 1996; MCEER/ATC 49-2 2003).

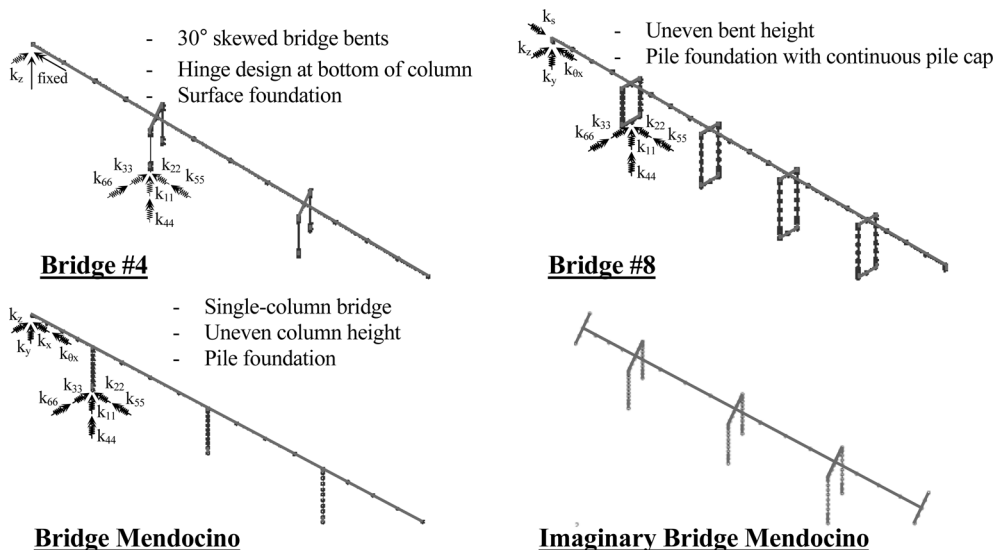


Fig. 8 The numerical models in ABAQUS for three prototype bridges

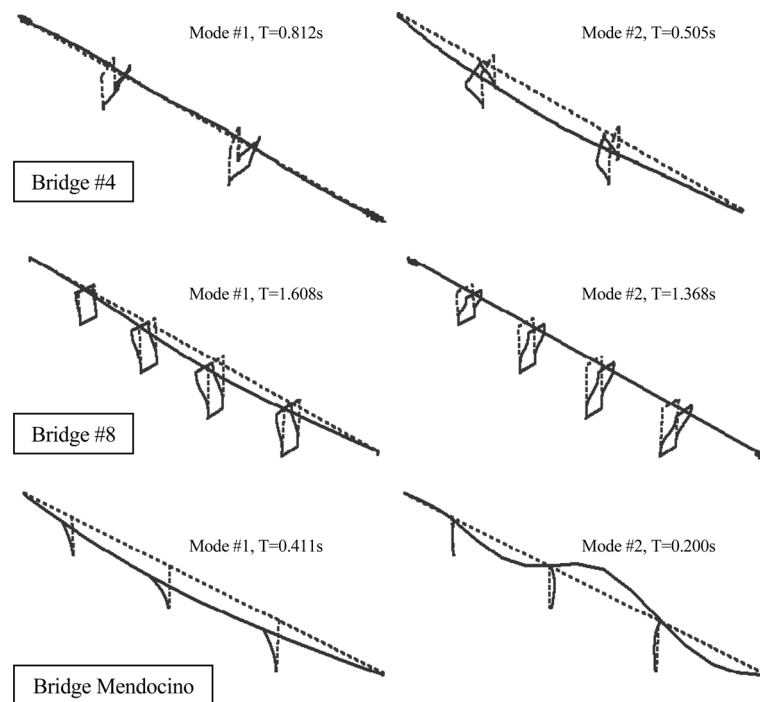


Fig. 9 First two mode shapes and natural periods of three prototype bridges

The nonlinear Timoshenko beam elements in ABAQUS utilize the user input nonlinear moment curvature relation with isotropic hardening rule to model the nonlinear flexural behavior of columns. For more accurate prediction of the seismic demands on the bridges, the columns can be modeled with the shear-flexural-interaction element (UEL springs) along the transverse and longitudinal directions, where the flexural and shear behavior are coupled together through equilibrium.

3.4 Nonlinear time history response analysis of bridges

The three-directional earthquake motions in Bin 4 corresponding to the hazard level of 2% probability of exceedance in 50 years are applied to the numerical models of prototype bridges and time history analyses were conducted to evaluate the seismic demands on bridges. Response quantities that are of interest are the maximum acceleration and column drift of bridges, and maximum sectional forces (i.e., axial, shear, bending moment) in columns. The issues investigated include: (a) effects of the ground motion intensity (e.g., PGA); (b) effects of vertical ground motions; (c) effects of nonlinear flexural behavior of columns; (d) effects of combined actions due to shear-flexural interaction; and (e) effects of structural properties.

Fig. 10 plots the maximum accelerations, maximum column drift, maximum column section forces and moments of Bridge #4 as function of PGA of the input motions using the nonlinear beam elements (hereafter referred to as the “nonlinear M- ϕ model”) for columns. It can be seen that with PGA increasing, the max acceleration and column drift also increase gradually; the section forces and section moments, on the other hand, have hit the capacity under these strong earthquakes (corresponding to hazard level of 2% probability of exceedance in 50 years) and thus remain almost

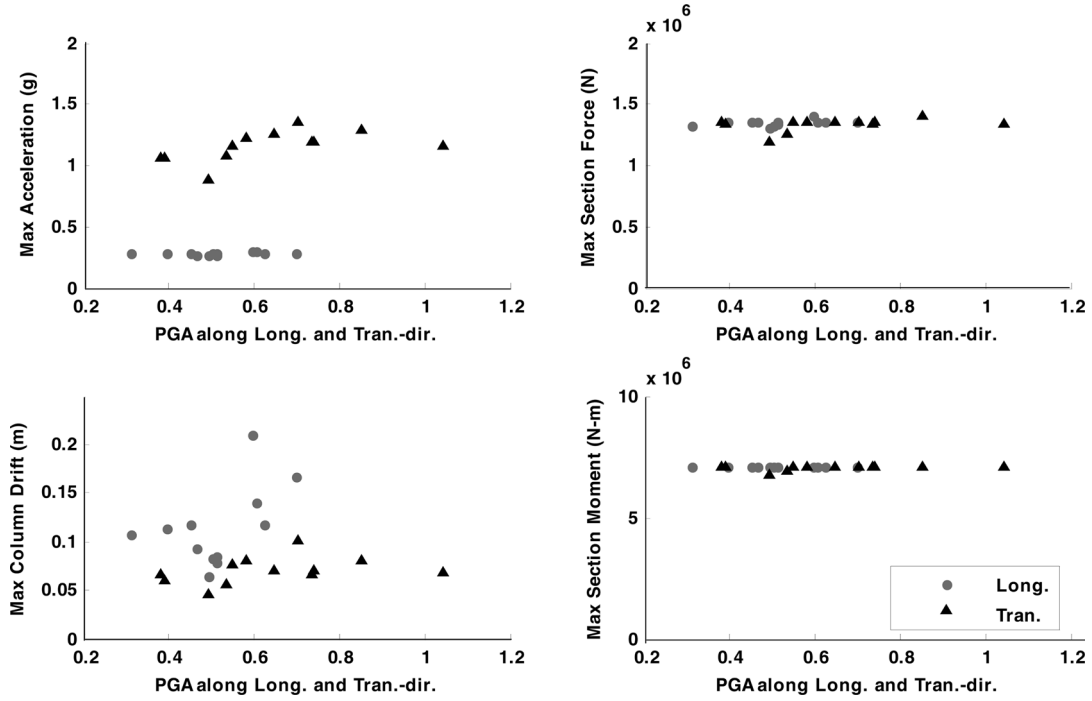


Fig. 10 Maximum response quantities of Bridge #4 using nonlinear beam elements for columns

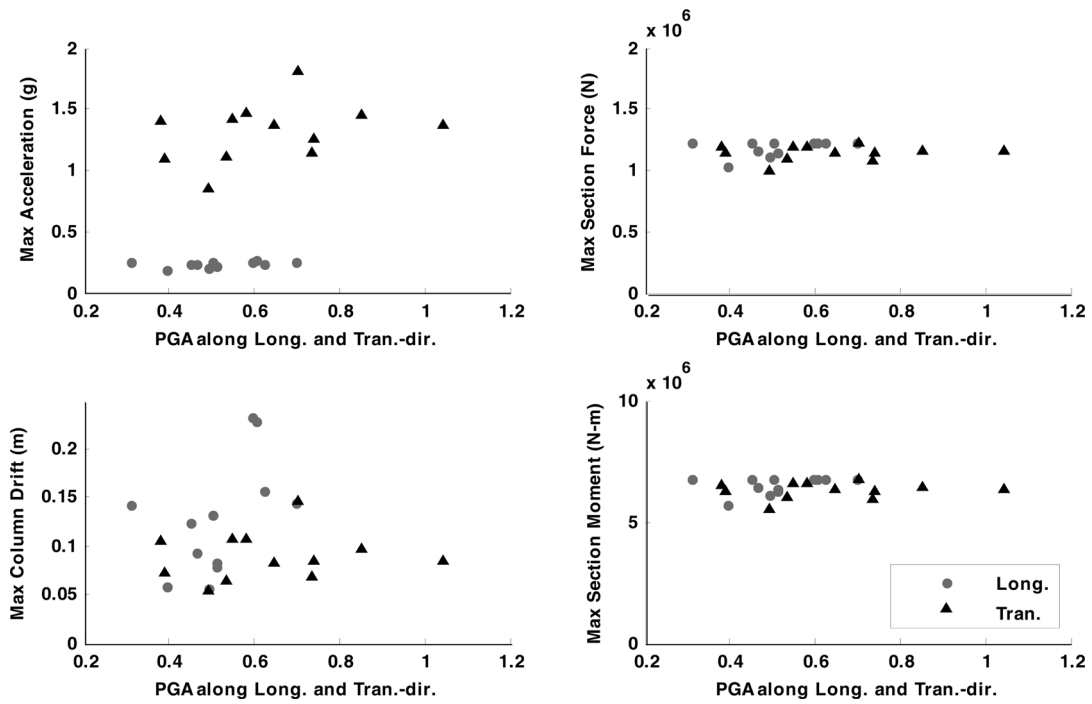


Fig. 11 Maximum response quantities of Bridge #4 using shear-flexural interaction user elements for columns

constant. Time history analyses were also conducted by inputting only the horizontal components of the ground motions to evaluate the effects of vertical ground motions. Due to the decoupled behavior of axial and flexural response in this model, it is found that the vertical ground motions do not affect the horizontal response quantities. Fig. 11 plots the response quantities (i.e., maximum accelerations, maximum column drift, maximum section forces and moments) of Bridge #4 as function of PGA of the input motions using the shear-flexural interaction user elements (hereafter referred to as the “UEL model”) for columns. It is noticed that all response quantities have experienced some change due to the consideration of the shear-flexural interaction of columns. Figs. 10 and 11 show that the bridge experiences larger displacement and smaller acceleration along the longitudinal direction because it is more flexible (due to free movement at abutment) than the transverse direction (shear keys prevent the movement at abutment). For Bridge #8 and Bridge Mendocino, the transverse direction experiences larger displacement but smaller acceleration because the response is dominated along this direction.

Fig. 12 compares the transverse and longitudinal column drift and section force time histories in Bent 3 of Bridge #8 computed by the nonlinear $M-\phi$ model and the UEL model. The results show that the UEL method yields larger column drift and smaller section forces than that of the nonlinear $M-\phi$ model. This is due to the consideration of shear-flexural interaction in the UEL model. The difference between these two models becomes more significant at larger displacement level as can be observed for the transverse direction in this case. Fig. 13 plots separately the shear and flexural responses of the same column using the UEL model, including the time histories of shear displacement, shear force, rotation, bending moment and the correspondent hysteresis loops when it is subject to earthquake motions recorded at Fletcher Drive station of the 1987 Whittier Narrows earthquake (see Table 5). It is seen that the developed shear-flexural interaction model and the

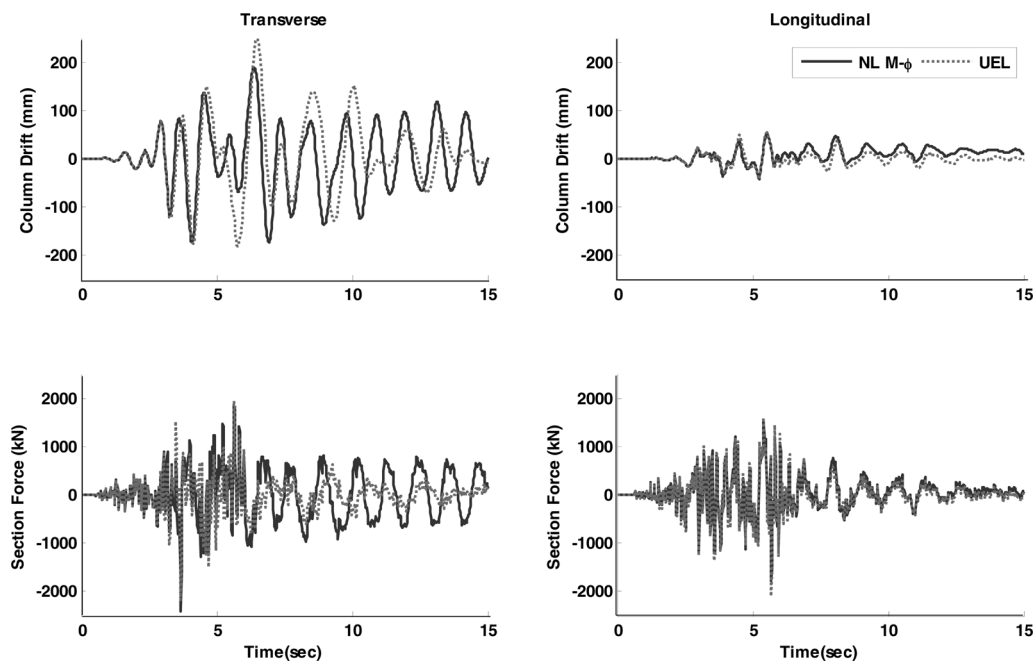


Fig. 12 Comparison of column drift and section force time histories in Bent 3 of Bridge #8, using nonlinear $M-\phi$ model and UEL model under 1987 Whittier Narrows earthquake

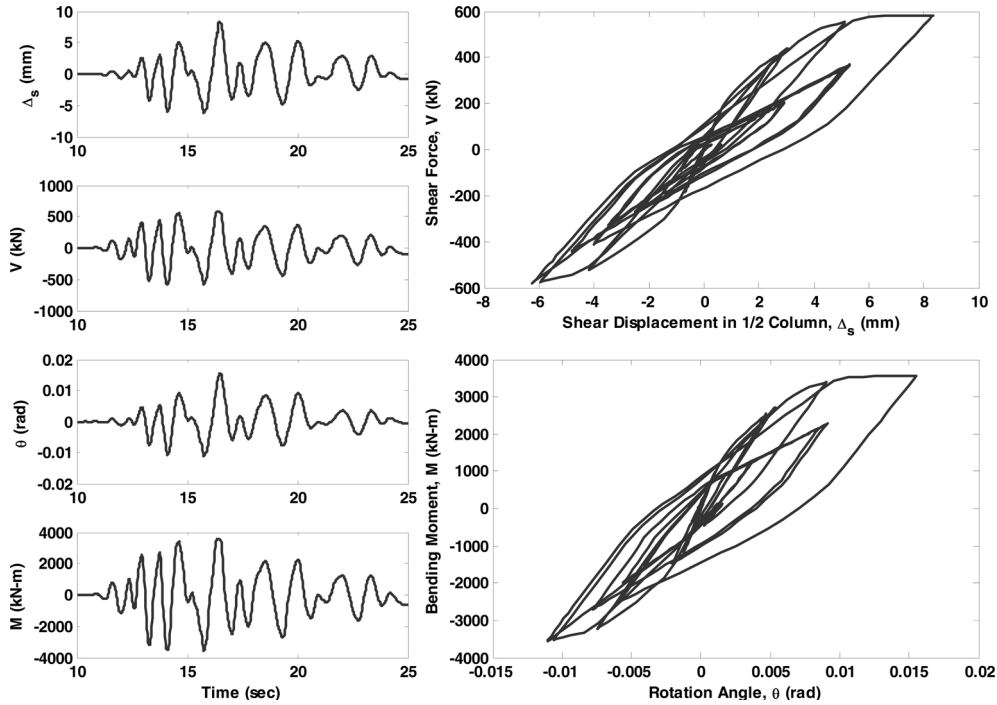


Fig. 13 Shear and flexural responses in Bent 3 of Bridge #8 using UEL model

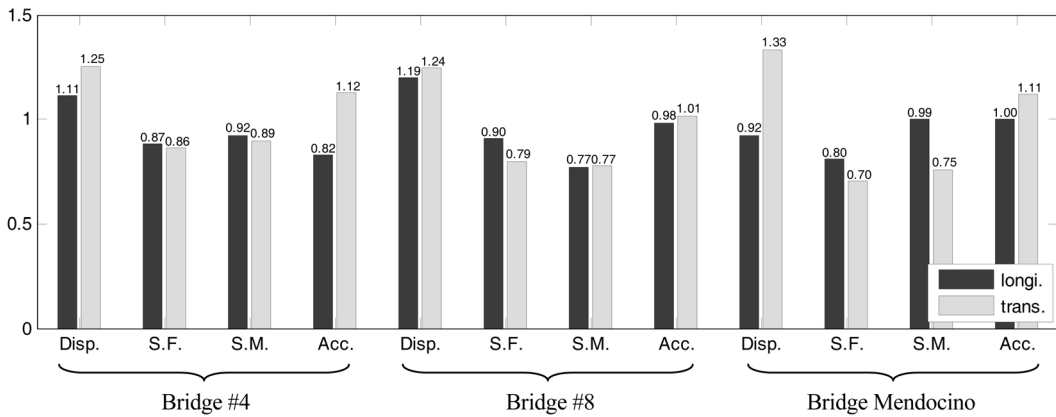


Fig. 14 Response ratio of UEL model to nonlinear M-φ model of three prototype bridges

implemented user element successfully model the nonlinear shear and flexural responses of the bridge (a MDOF system) under seismic loading.

Fig. 14 summarizes the average bridge response quantities obtained by using shear-flexural interaction user elements for columns (UEL model) normalized by those derived from the nonlinear M-φ model (i.e., Fig. 11 normalized by Fig. 10) for all three prototype bridges. It can be seen that considering shear-flexural interaction of columns results in larger drift demand and smaller section forces and section moments for all three bridges, despite their different structural and geometry characteristics.

Table 6 Moments, torsional moments and T/M ratios of different bridge models

Bridge Model	M_1 (Trans.)	M_2 (Long.)	T	T/M_1	T/M_2
Bridge #4	7.05	7.02	0.0008	0.0001	0.0001
Bridge #8	7.77	10.1	0.418	0.056	0.042
Mendocino (a)	1.71	7.74	0.840	0.517	0.109
Mendocino (b)	1.82	7.60	1.250	0.693	0.164
Mendocino (c)	2.06	6.86	0.389	0.194	0.056
Mendocino (d)	2.07	6.22	0.306	0.163	0.049

Notes Bridge Mendocino (a): single column and straight; (b) single shorter column and straight; (c) bent column and straight; (d) bent column and skew. All units for M_1 (transverse), M_2 (longitudinal) and T are MN·m

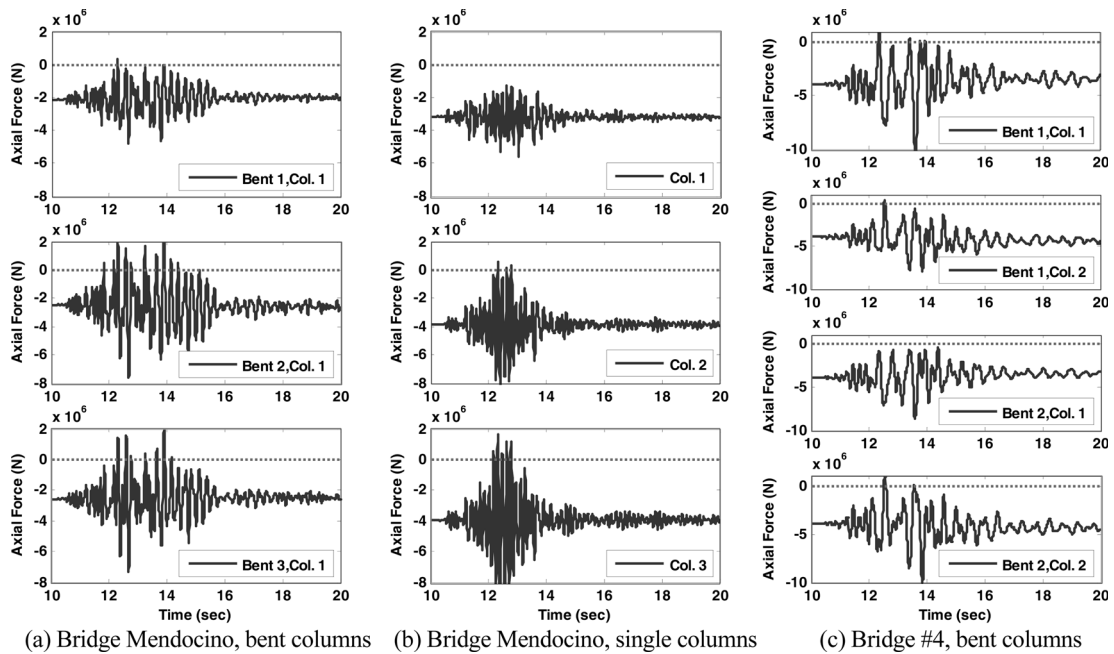


Fig. 15 Observed tensile axial forces in bent-column and in single-column design bridges

During the analysis, the maximum torsion to maximum moment ratios (T/M ratios) in columns are also monitored to evaluate the effects of different geometric characteristics. Table 6 lists the averaged maximum moments, torsional moments and T/M ratios of different bridge models. Four different variations of the Mendocino Bridge are considered to evaluate the effects of (1) shorter column; (2) single vs. bent column design; (3) skew vs. straight design. It has been observed that a relatively stiffer or short column in the bridges will introduce a higher level of asymmetry into the system and thus results in higher T/M ratios. It has also been found that pinned design at the column bases (Bridge #4) greatly eliminates the torsion moment demands in the columns. Nevertheless, pinned base design will change the deformed shape of the column from double curvature to single curvature, resulting in a softer (larger lateral displacement) and weaker (lower shear capacity) bridge pier given

the same column cross section. Besides, the numerical results shows that skewed bents in the bridges do not necessarily induce higher level of T/M ratio into the columns.

Finally, it has been found that bridges with single-column design in general will experience less tensile axial force in the columns than bridges with bent-column design. Fig. 15 shows the axial force time histories in all columns of the imaginary and original Bridge Mendocino, and the Bridge #4. It can be seen that the columns in the imaginary Bridge Mendocino [case (a), bent-column design] undergo more tensile axial force than the original bridge [case (b), single-column design] owing to its lower initial compressive axial load level. Tensile axial force is harmful to the RC columns since it will reduce the shear capacity and exacerbate the lateral deformation of the columns, as has been shown in Fig. 3. Bent-column design, however, is not necessarily bad if the initial compressive axial force level is high enough to prevent it from going into the tension side [case (c), bent-column design].

4. Conclusions

This paper evaluates the seismic response of three prototype reinforced concrete bridges under earthquake shakings using comprehensive numerical models that are capable of simulating the complex soil-structural interaction effects and nonlinear behavior of columns. An analytical approach that can capture the shear-flexural interacting behavior of columns is implemented as user element in software ABAQUS to model the realistic nonlinear behavior due to combined actions of shear force, axial force and bending moment. Seismic response analyses were conducted on the prototype bridges under suites of ground motions that correspond to the severe hazard level of 2% probability of exceedance in 50 years at a specific site in Southern California. The response quantities including column drift, acceleration, section force and section moment etc. were derived and compared among three prototype bridges to evaluate the effects of structural characteristics and the shear-flexural interaction of columns on seismic demand of bridges. It is found that the responses of bridges are correlated well with the intensity of the input ground motions, i.e. PGA. The vertical input motions have resulted in much larger responses in vertical direction; sometimes even introduce tension in columns. The shear-flexural interaction of columns results in larger displacement demand on bridge columns and smaller section shear force and moment. The detailed responses depend greatly on the structural and geometric characteristics of the bridge. The bridge responses differ in longitudinal and transverse directions because of their different force-resisting mechanism.

Acknowledgements

The research presented here was funded by National Science Foundation through the Network for Earthquake Engineering Simulation Research Program, grant CMMI-0530737, Joy Pauschke, program manager. Dr. Christine Goulet offered valuable help in selecting earthquake motions based on Probabilistic Seismic Hazard Analysis and the hazard level at target periods. Dr. David H. Sanders provided the shaking table test results for model calibration.

References

- ABAQUS (2003), ABAQUS Inc., Providence, RI.
- Calderone, A.J., Lehman, D.E. and Moehle, J.P. (2000), *Behavior of Reinforced Concrete Bridge Columns Having Varying Aspect Ratios and Varying Lengths of Confinement*, Report No. PEER-00/08, Pacific Earthquake Engineering Research Center, University of California, Berkeley.
- ElMandooh Galal, K. and Ghobarah, A. (2003), "Flexural and shear hysteretic behavior of reinforced concrete columns with variable axial load", *Eng. Struct.*, **25**(11), 1353-1367.
- FHWA (1996), *Seismic Design of Bridges: Design Example No. 4 - Three Span Continuous CIP Concrete Bridge*, Publication No. FHWA-SA-97-009, Federal Highway Administration, Washington, D.C.
- Gazetas, G. (1991), "Formulas and charts for impedances of surface and embedded foundations", *J. Geotechnical Eng.*, **117**(9), 1363-1381.
- Goulet, C.A., Haselton, C.B., Mitrani-Reiser, J., Beck, J.L., Deierlein, G., Porter, K.A. and Stewart, J.P. (2007), "Evaluation of the seismic performance of a code-conforming reinforced-concrete frame building - from seismic hazard to collapse safety and economic losses", *Earthq. Eng. Struct. Dyn.*, **36**(13), 1973-1997.
- Hsu, Y.T. and Fu, C.C. (2004), "Seismic effect on highway bridges in chi chi earthquake", *J. Perform. Constr. Fac.*, **18**(1), 47-53.
- Laplace, P., Sanders, D., Saiidi, M.S. and Douglas, B. (1999), *Shake Table Testing of Flexure Dominated Reinforced Concrete Bridge Columns*, Report No. CCEER 99-13, Center for Earthquake Engineering Research, University of Nevada, Reno.
- Lehman, Dawn E. and Moehle, Jack P. (2000), *Seismic Performance of Well-confined Concrete Bridge Columns*, Report No. PEER-98/01, Pacific Earthquake Engineering Research Center, University of California, Berkeley.
- Makris, N. and Gazetas, G. (1993), "Displacement phase differences in a harmonically oscillating pile", *Geotechnique*, **XLIII**(1), 135-150.
- Mazzoni, S., McKenna, F., Scott, M.H. and Fenves, G.L. (2006), *Open System for Earthquake Simulation (OpenSees) Command Language Manual*, Pacific Earthquake Engineering Research Center, University of California, Berkeley.
- MCEER/ATC 49-2 (2003), *Design Examples: Recommended LFRD Guidelines for the Seismic Design of Highway Bridges*, Rep. No. MCEER/ATC 49-2, ATC/MCEER Joint Venture.
- Mostafaei, H. and Kabeyasawa, T. (2007), "Axial-shear-flexural interaction approach for reinforced concrete columns", *ACI Struct. J.*, **104**(2), 218-226.
- Ozcebe, G. and Saatcioglu, M. (1989), "Hysteretic shear model for reinforced concrete members", *J. Struct. Eng.*, **115**(1), 132-148.
- RESPONSE-2000, <http://www.ecf.utoronto.ca/~bentz/home.shtml>, last accessed August 2008.
- Saadeghvaziri, M.A. and Foutch, D.A. (1991), "Dynamic behavior of R/C highway bridges under the combined effect of vertical and horizontal earthquake motions", *Earthq. Eng. Struct. Dyn.*, **20**(6), 535-549.
- Saatcioglu, M. and Ozcebe, G. (1989), "Response of reinforced concrete columns to simulated seismic loading", *ACI Struct. J.*, **86**(1), 3-12.
- Sakai, J. and Kawashima, K. (2000). *Effect of Varying Axial Loads Including a Constant Tension on Seismic Performance of Reinforced Concrete Bridge Columns*, Tokyo Institute of Technology, Tokyo, Japan.
- Seible, F. and Priestley, M.J.N. (1999), "Lessons learned from bridge performance during Northridge earthquake", *Seismic Response of Concrete Bridges*, 29-55, ACI International, Farmington Hills, MI.
- Sezen, H. (2008), "Shear deformation model for reinforced concrete columns", *Struct. Eng. Mech.*, **28**(1), 39-52.
- Stewart, J.P., Comartin, C. and Moehle, J.P. (2004), "Implementation of soil-structure interaction models in performance based design procedures", *Proc. 13th World Conference on Earthquake Engineering*, Vancouver, Canada.
- Vecchio, F.J. and Collins, M.P. (1986), "Modified compression-field theory for reinforced concrete elements subjected to shear", *J. Am. Con. Inst.*, **83**(2), 219-231.
- Wolf, J.P. (1997), "Spring-dashpot-mass models for foundation vibrations", *Earthq. Eng. Struct. Dyn.*, **26**(9), 931-949.
- Xu, S. and Zhang, J. (2008), "Hysteretic models for reinforced concrete columns considering axial-shear-flexural interaction", *Proc. 14th World Conference on Earthquake Engineering*, Paper ID: S16-01-011, Oct. 12-17,

Beijing, China.

- Yoneda, K., Kawashima, K. and Shoji, G. (2001), "Seismic retrofit of circular reinforced bridge columns by wrapping of carbon fiber sheets", *Proc. JSCE*, **682**, 41-56.
- Zhang, J. and Makris, N. (2002a), "Kinematic response functions and dynamic stiffnesses of bridge embankments", *Earthq. Eng. Struct. Dyn.*, **31**(11), 1933-1966.
- Zhang, J. and Makris, N. (2002b), "Seismic response analysis of highway overcrossings including soil-structure interaction", *Earthq. Eng. Struct. Dyn.*, **31**(11), 1967-1991.